

# Application of geotechnical LRFD for ground improvement by Deep Mixing Method in Korea

Yeon-Soo Jang

Professor, Dept. of Civil & Environ. Eng., Dongguk University, Seoul, Korea, ysjang@dongguk.edu

Jun-Mo Park

Senior Engineer, Geotechnical Division, Kun-Il Engineering Co., Seoul, Korea

Tae-Seon Yang

Professor, Dept. of Civil Engineering, Kimpo University, Gyeonggi Province, Korea

**KEYWORDS:** Load and Resistance Factor Design, Ground Improvement, Deep Mixing Method, Reliability Based Design, Limit State Design

**ABSTRACT:** To prepare the global standardization of the geotechnical method, i.e. AASHTO LRFD, Euro code 7, several research studies for applying the LRFD method to geotechnical engineering based on the reliability approach progress actively in Korea. In this study, the geotechnical LRFD is applied in the area of soil improvement, i.e. deep mixing method (DMM). The resistance bias factor is calculated from the ratio of the unconfined compressive strength on in-situ stabilized soil column to the design standard strength of the treated soil manufactured in the laboratory. Then, the resistance factor is obtained after calculating the resistance bias factors. The target reliability indices for calculating the resistance factors are determined by performing the reliability analyses using the various design cases of the DMM. From the analyses, the bias factor and the COV of the resistance are calculated as  $\lambda_R=1.36$  and  $COV_R=0.35$ . The dominant failure modes in the DMM improved ground are the compressive strength at the toe of the improved ground and the shear strength of the improved ground. The target reliability index is suggested as  $\beta_T=3.1$  and the resistance index for internal stability of the improved ground is calculated as  $\phi=0.43\sim 0.44$ . It is expected that the suggested resistance factors would be useful for the geotechnical engineers to design the port and harbor structures on the DMM improved grounds which have large uncertainties of the random variables in load and resistance.

## 1 INTRODUCTION

Recently, the limit state design (LSD) and the load resistance factor design (LRFD) becomes the standardized method in geotechnical engineering, and the criteria of the geotechnical design begin to transfer from the allowable stress design to LRFD. In EU countries, e.g. Belgium (NBN EN 2005), Denmark (DS/EN 2007), France (NF EN 2005), German (DIN EN 2009), adopted Eurocode 7 (CEN 2004) based on the limit state design. In North America, US (AASHTO 2010) and Canada (CSA 2006) adopted the LRFD method. In Asian countries, limit state design method is selected in China (Zhang et al. 2003) and Japan (Okahara et al. 2003) which is similar to Eurocode 7.

LRFD has been used in North America for the design of highway bridges and their substructures. LRFD, which accounts for uncertainty in load and resistance separately, can handle the design uncertainty in a more systematic manner than ASD (Allowable stress design) method. LRFD is known to provide more consistent levels of safety across the entire structure by calibrating the

parameters with respect to the actual load and the resistance data as well as using reliability based resistance factors.

LRFD to bridge substructures components has been applied for shallow foundations (Fellenius 1994, Meyerhof 1994, Paikowsky et al. 2010), deep foundations (O'Neill 1995, Paikowsky et al. 2004), foundation of offshore platforms (Hamilton & Murff 1992, Tang 1993), retaining wall and mechanically stabilized earth (MSE) walls (Withiam et al. 1995, D'Appolonia 1999, Chen 2000a, Chen 2000b, Allen et al. 2001, Huang 2010), and soil-nailing (Lazarte 2011).

In Korea, LRFD was introduced in the standard specifications of highway bridges in 1996 and the reliability based design method is first applied to the performance-based seismic design in 1998. Most of the LRFD applications in geotechnical engineering in Korea have been performed in the area of the driven piles (Kwak et al. 2010, Kim & Lee 2012) and in-situ installed pile methods (Yoon et al. 2007). Korea Institute of Construction Technology has performed the R&D entitled "Determination of resistance factors for foundation structure design by LRFD (KICT 2008)" and the result was adopted in the design specifications of structural foundation (KGS 2009). Currently, the grounds modified by various soil improvement methods are used for foundations of the structures in Korea. However, the applications of LRFD for those soils are quite rare.

The authors have been performed the studies for applying the LRFD method to weak soil improvement method and for modifying the standards of the foundation design conforming to the world geotechnical standards. In this paper, the resistance factors of LRFD are suggested for the foundations improved by the deep mixing method (DMM). The resistance bias factor is calculated from the ratio of the unconfined compressive strength of the core samples from the in-situ stabilized column to the design standard strength of the treated soil manufactured in the laboratory. The resistance factors are obtained after calculating the resistance bias factors. The target reliability indices for calculating the resistance factors are determined by performing the reliability analyses using the various design cases of the DMM and by the literature studies.

## 2 THEORETICAL BACKGROUND OF LRFD

In the LRFD method, two parameters are used to account for the uncertainty, i.e. load factors for load uncertainty and resistance factors for the material uncertainty (Equation 1). In the equation, the resistance capacity which is obtained by multiplying nominal resistance,  $R_n$ , to the resistance factor,  $\phi$ , is greater or equal to the design loads which is calculated by the nominal load,  $Q_n$ , times to the load factor,  $\gamma_Q$ , and the load modifier factor,  $\eta_i$  (AASHTO 2010).

$$\phi R_n \geq \sum_{i=1}^N \gamma_i \eta_i Q_i \quad (1)$$

The load (Q) and the resistance (R) in the Equation 1 are the random variables and are represented by the probability density curve of normal or lognormal distributions (Figure 1a). The hatched area in Figure 1a represents the probability of failure in which the load becomes greater than the resistance. To calculate the probability of failure, the double integration is needed with respect to the load and the resistance. Therefore, the integral equation is transformed to the limit state function  $g(=R-Q)$  and the probability of failure is calculated using Equation 2. Figure 1b shows the failure region,  $g < 0$ .  $P_f$  is again showed by the reliability index,  $\beta$ . Reliability index,  $\beta$  is the distance of  $\mu_g$  normalized by the standard deviation of R-Q,  $\sigma_g$ .

$$P_f = P(R - Q \leq 0) = P(g \leq 0) = P(-\beta) \quad (2)$$

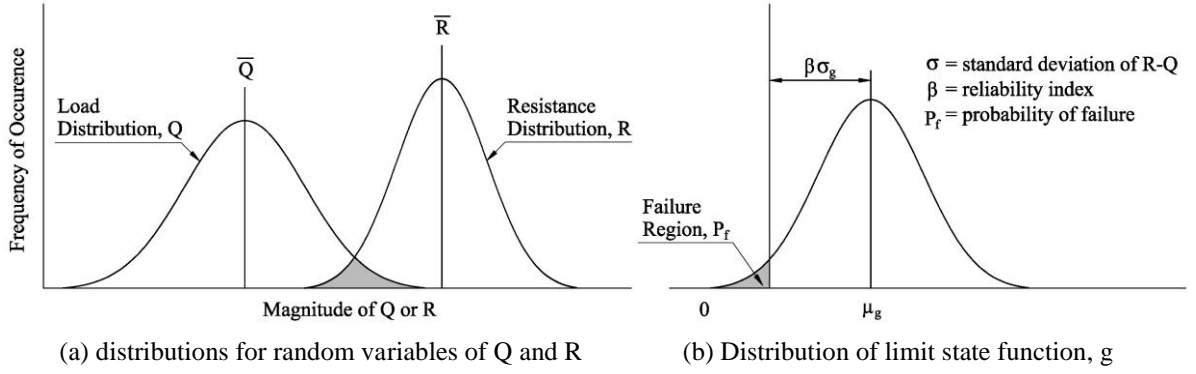


Figure 1. Description of the Probability of failure and reliability index (Allen et al. 2005).

Nominal values of load and resistance has the relation of Equation 3 and 4, in which  $\lambda_Q$  and  $\lambda_R$  are the bias factors of Q and R. Bias factors are represented by the ratio of the measured values with the predicted values of Q and R. Bias factors give the clue to judge the accuracy of the analysis models for Q and R.

$$Q_m = \lambda_Q Q_n \quad (3)$$

$$R_m = \lambda_R R_n \quad (4)$$

When the Q and R have the normal distributions, the reliability index,  $\beta$  in Figure 1b is represented by Equation 5. In the case that Q and R has lognormal distributions, the reliability index,  $\beta$  is shown as the Equation 6. Probability of failure in Equation 2 is represented again as Equation 7 using the reliability index,  $\beta$ .

$$\beta = \frac{\mu_g}{\sigma_g} = \frac{R_m - Q_m}{\sqrt{\sigma_R^2 + \sigma_Q^2}} \quad (5)$$

$$\beta = \frac{\ln \left[ (R_m / Q_m) \sqrt{(1 + COV_Q^2) / (1 + COV_R^2)} \right]}{\sqrt{\ln \left[ (1 + COV_Q^2)(1 + COV_R^2) \right]}} \quad (6)$$

$$P_f = 1 - \Phi(\beta) \quad (7)$$

where  $COV_Q$  and  $COV_R$  are the coefficient of variance for load and resistance, Q and R.

The resistance factor is derived as Equation 8 including the dead and live load from Equation 1 and the target reliability index from Equation 6 (Barker et al. 1991, Withiam et al. 1998, Paikowsky et al. 2004).

$$\phi = \frac{\lambda_R \left( \gamma_{QD} \frac{Q_D}{Q_L} + \gamma_{QL} \right) \sqrt{\frac{1 + COV_{QD}^2 + COV_{QL}^2}{1 + COV_R^2}}}{\left( \lambda_{QD} \frac{Q_D}{Q_L} + \lambda_{QL} \right) \exp \left( \beta_T \sqrt{\ln \left[ (1 + COV_R^2)(1 + COV_{QD}^2 + COV_{QL}^2) \right]} \right)} \quad (8)$$

in which  $\phi$  is the resistance factor,  $\lambda_R$ ,  $\lambda_{QD}$ ,  $\lambda_{QL}$  are the bias factors of the resistance, the dead and the live load, respectively.  $\gamma_{QD}$ ,  $\gamma_{QL}$  are the dead and the live load factors, and  $COV_R$ ,  $COV_{QD}$ ,  $COV_{QL}$  are the coefficient of variation of the resistance, the dead and the live loads, respectively.  $Q_D/Q_L$  is the ratio of the dead and live load, and  $\beta_T$  is the target reliability index.

The procedure of studying the geotechnical LRFD in this study is the following:

- 1) The field data of the design parameters are collected and analyzed statistically. The bias factors are obtained for the field data versus the predicted data using the design formula.
- 2) The limit state functions of the structures of interest are defined for the possible failure modes.
- 3) The allowable level of the uncertainty is decided from the reliability analysis and is shown by the target reliability index.
- 4) The calibrations of the resistance factors for the internal stability failure modes of the DMM improved harbor structures are performed.

### 3 BASIC CONCEPT AND DESIGN PROCEDURE OF DMM

Deep Mixing Method (DMM) is one of the soil improvement method in which the stabilizers, e.g. lime and cement etc., are supplied into the ground and forcefully mixed with the weak soils for the purpose of increasing the strength and decreasing the settlement of the ground. The stabilizer mixed with the weak soil incurs the chemical reactions named as pozzolanic reaction.

The types of foundation structures made by DMM are divided into the block, wall, group column-type structures and are made according to the various ground conditions and the foundations of the super-structures (Figure 2). In Scandinavia and USA, the group column-type DMM is applied to support embankments and light weight superstructures. In Korea and Japan, the wall-type improvements are preferred as the foundation of harbor and port structures where the weights of superstructures are supported by the improved ground.

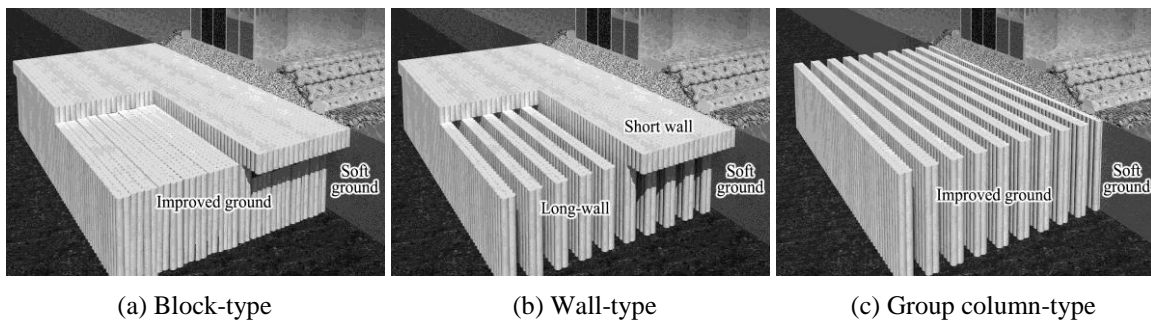


Figure 2. Improvement patterns for Deep Mixing Method.

The procedure of DMM design is the followings and the details are found in CDIT (2002).

- Step 1 : By assuming the improved grounds can support the upper structures in full, the external stability of the structures is checked for the failure modes of the sliding, the overturning and the bearing capacity of the ground.
- Step 2 : The internal stability is checked for the stresses developed by the external stresses. The items of the internal stability checks are toe pressures of the improved ground, shear stress of long-wall and short-walls and the extrusion failure of untreated soil.
- Step 3 : The circular sliding failure of the combined structure and foundation, and the settlement of the improved ground are checked.

## 4 STATISTICAL ANALYSIS AND CALIBRATION OF DEEP MIXING FOUNDATION

### 4.1 DATABASE OF DMM

Compressive strength of the improved grounds using DMM is very important for securing the stability of the structures of interest. In this study, the compressive strength data of the DMM are collected from the laboratory tests. The laboratory DMM samples are produced in the process of the quality control and quality assurance of the mix design (Table 1). Also, the in-situ samples collected from the field soil improvement by DMM (Table 2). The data of the compressive strength for both the laboratory and field samples are obtained from the six construction sites improved by DMM (Table 1 & 2). The resistance bias factors are calculated from the statistical analysis of the above DMM data.

The average compressive strength of the field samples,  $q_{uf}$ , is in the range of 1,737~3,953kPa and estimated as 85% of those obtained from the laboratory mixed DMM samples,  $q_{ul}$  (Figure 3) in this study. These results are a little lower than the ratios of the compressive strength of DMM,  $q_{uf} / q_{ul} = 1.0$  suggested in Japan (CDIT 2002).

Table 1. Unconfined compression strength data for laboratory test for mix design

| Site                        | Mixing conditions                   |                         | Laboratory Strength<br>$q_{ul}$ (kPa) | Design Standard Strength<br>$q_{uck}$ (kPa) |
|-----------------------------|-------------------------------------|-------------------------|---------------------------------------|---|
|                             | Cement rate<br>(kg/m <sup>3</sup> ) | Water/Cement ratio(w/c) |                                       |   |
| A Daebyun fishing port      | 300                                 | 0.8                     | 3,380                                 | 2,253                                       |
| B Seoul-Incheon waterway    | 300                                 | 0.8                     | 5,465                                 | 3,643                                       |
| C Busan breakwater          | 180                                 | 0.8                     | 2,711                                 | 1,807                                       |
|                             | 200                                 | 0.8                     | 3,649                                 | 2,433                                       |
|                             | 220                                 | 0.8                     | 4,227                                 | 2,818                                       |
| D Yeosu port access road    | 250                                 | 0.8                     | 2,183                                 | 1,455                                       |
| E Yongho bay reclaimed land | 250                                 | 1.0                     | 4,038                                 | 2,692                                       |
|                             | 300                                 | 0.9                     | 4,510                                 | 3,007                                       |
| F Busan container terminal  | 270                                 | 0.8                     | 4,357                                 | 2,905                                       |
| G Ulsan south breakwater    | 300                                 | 0.7                     | 4,850                                 | 3,233                                       |

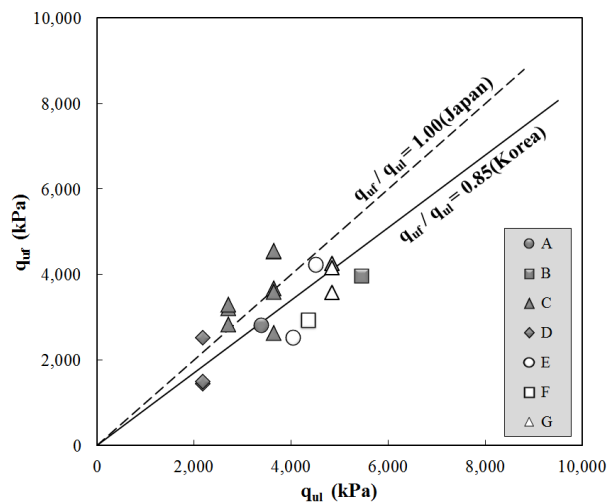


Figure 3. Relationship between unconfined compression strength of laboratory treated soil and of in-situ improved soil.

The coefficient of variations (COVs) of the compressive strength of the in-situ samples,  $q_{uf}$ , are in the range of 0.227~0.365. These are similar to the ranges of COVs suggested by Suzuki (1982), Kawasaki et al. (1984) and Taki (2003). The average of the COVs for all  $q_{uf}$  in Table 2 is analyzed as 0.340.

Table 2. Unconfined compression strength data for in-situ core samples

| Site                        | Unconfined compression strength( $q_{uf}$ ) for in-situ core samples |               |           |       |
|-----------------------------|--|---------------|-----------|-------|
|                             | Num. of data   | Range(kPa)    | Mean(kPa) | COV   |
| A Daeyun fishing port       | 4  | 2,224 ~ 4,184 | 2,816     | 0.326 |
| B Seoul-Incheon waterway    | 3  | 3,080 ~ 4870  | 3,953     | 0.227 |
| C Busan breakwater          | 68   | 1,042 ~ 5,597 | 3,257     | 0.335 |
| D Yeosu port access road    | 12   | 943 ~ 2,895   | 1,737     | 0.354 |
| E Yongho bay reclaimed land | 4  | 2,061 ~ 4,836 | 3,378     | 0.340 |
| F Busan container terminal  | 15   | 1,698 ~ 4,265 | 2,786     | 0.301 |
| G Ulsan south breakwater    | 44   | 1,450 ~ 6,549 | 3,585     | 0.365 |
| All                         | 150  | 943 ~ 6,549   | -         | 0.340 |

#### 4.2 RESISTANCE BIAS FACTOR

The statistical characteristics of loads which transferred to the foundations can be brought from the LRFD design standards for the superstructures. Hence, the load factors and the load bias factors used in the formula of resistance calculation (Equation 8), can be presumed as the determined values from the standards. The statistical characteristics of resistance factors are estimated as the bias factors and COVs of resistance factors within the allowable ranges of load ratio ( $Q_D / Q_L$ ) (Nowak 1999; Paikowsky et al. 2010).

The bias factor of the resistance of the DMM improved grounds can be defined as the ratio of the design standard strength ( $q_{uck}$ ) predicted from the compressive tests for the laboratory manufactured samples and those of the core samples from the field ( $q_{uf}$ ). It can be written as Equation 9 from the derivation of Equation 3 & 4.

$$\lambda_R = \frac{R_m}{R_n} = \frac{q_{uf}}{q_{uck}} \quad (9)$$

The bias factors and COVs for the cases of DMM construction sites in Table 1 & 2 are calculated as  $\lambda_R = 0.45 \sim 2.35$  and  $COV_R = 0.237 \sim 0.35$  (Table 3).

Table 3. Statistics of biases for unconfined compression strength

| Site                        | Resistance bias parameters |              |             |         |
|-----------------------------|----------------------------|--------------|-------------|---------|
|                             | Num. of data               | Biases range | $\lambda_R$ | $COV_R$ |
| A Daeyun fishing port       | 4                          | 0.99 ~ 1.86  | 1.25        | 0.33    |
| B Seoul-Incheon waterway    | 3                          | 0.85 ~ 1.34  | 1.09        | 0.23    |
| C Busan breakwater          | 60                         | 0.74 ~ 2.35  | 1.56        | 0.29    |
| D Yeosu port access road    | 12                         | 0.65 ~ 1.99  | 1.19        | 0.35    |
| E Yongho bay reclaimed land | 4                          | 0.77 ~ 1.61  | 1.17        | 0.30    |
| F Busan container terminal  | 15                         | 0.58 ~ 1.47  | 0.96        | 0.30    |
| G Ulsan south breakwater    | 43                         | 0.45 ~ 1.92  | 1.09        | 0.35    |

|     |     |             |      |      |
|-----|-----|-------------|------|------|
| All | 150 | 0.45 ~ 2.35 | 1.36 | 0.35 |
|-----|-----|-------------|------|------|

In all sites except the site F, the bias factors of resistance are calculated greater than 1.0. It can be recognized that the predicted compressive strengths are tend to be underestimate the compressive strength of field core samples. The average value of the bias factors and COVs for all cases are calculated as  $\lambda_R=1.36$ , and  $COV_R=0.35$ .

In order to find the distribution types of the resistance bias, they are plotted in normal probability paper for the sites of C and G where the data numbers are more than 30 (Figure 4). The theoretical distribution curves of lognormal and normal distributions are shown as the solid and the dotted lines, respectively, in the same figure. It was found that the distributions of the bias factors of resistance are well fitted into both curves, although the distributions of the resistance bias are assumed as the lognormal in LRFD.

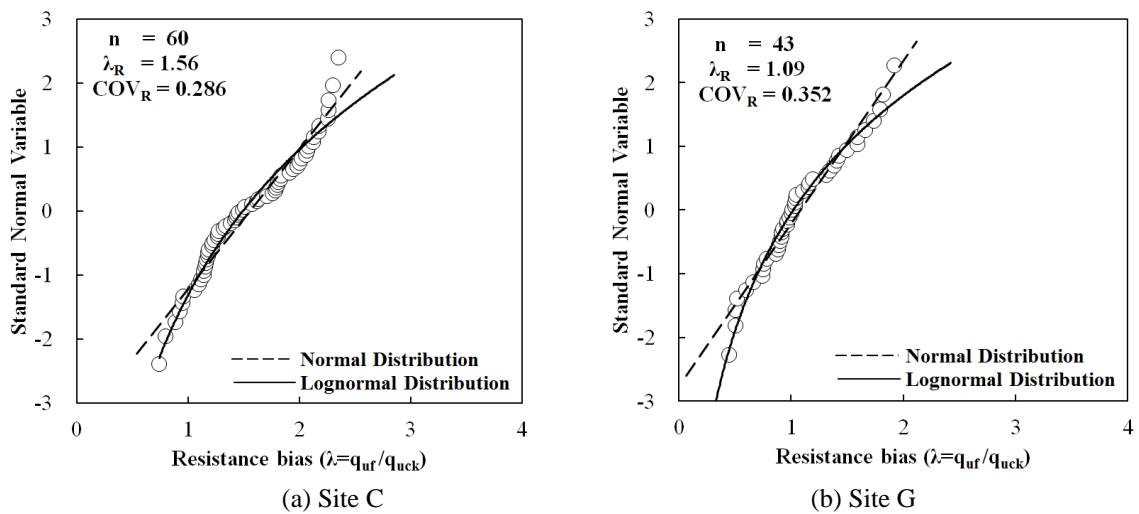


Figure 4. Standard normal variable of the resistance biases.

The goodness-of-fit (GOF) tests, i.e. Kolmogorov-Smirnov test and Chi-square test, have been carried out to estimate the fit of the distribution of the resistance bias to the theoretical normal and lognormal distributions. They are performed for the significance level 5% and the results are shown Table 4. The tested statistic values are satisfied for the data of the Site C and G to both normal and lognormal distributions, since the values are well within the critical values. For site C, the tested statistic value is lower in the case of the normal distribution meaning that the data are more fitted to the normal distribution. For the site G, the data are more fitted to the lognormal distribution. The histogram of the resistance bias is plotted along with the probability density distribution curves of normal and lognormal distribution curves in Figure 5 for the data of Site C and G.

Table 4. Statistical verification of bias factors for unconfined compression strength of DMM samples

| Site | Kolmogorov-Smirnov Test |                     |                | Chi-square Test        |                     |                |
|------|-------------------------|---------------------|----------------|------------------------|---------------------|----------------|
|      | Test statistics         |                     | Critical value | Test statistics        |                     | Critical value |
|      | Lognormal distribution  | Normal distribution |                | Lognormal distribution | Normal distribution |                |
| C    | 0.102                   | 0.095               | 0.172          | 3.131                  | 2.121               | 9.488          |
| G    | 0.087                   | 0.159               | 0.198          | 5.261                  | 4.230               | 9.488          |

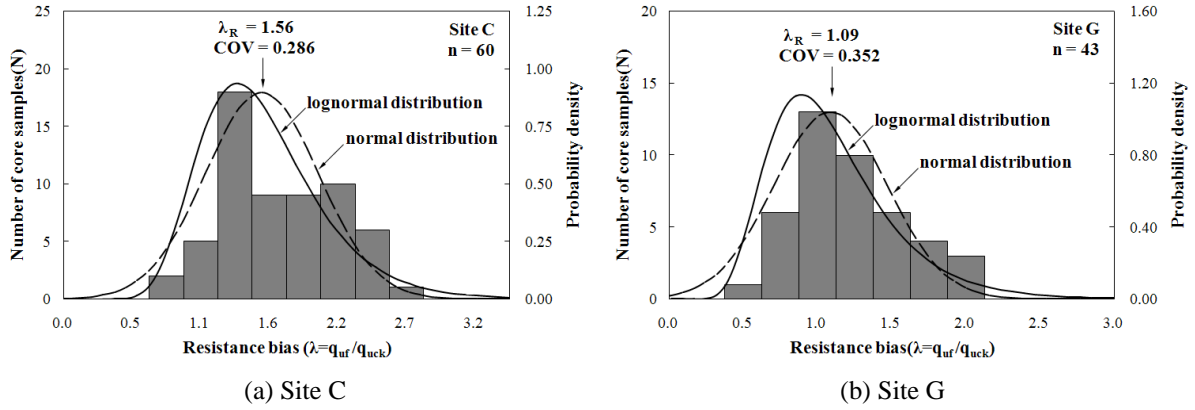


Figure 5. Histogram and probability density function of the biases.

## 5 RELIABILITY ANALYSIS

The resistance factors of LRFD in geotechnical engineering in 1990s were calibrated by fitting to the safety factors of ASD (allowable stress design) due to the lack of statistical data of geotechnical parameters. Most of the random variables used at this period were assumed to have lognormal distributions. Kulhawy & Phoon (2002) suggested the calibration of design parameters according to the reliability-based design rather than to the basis of safety factors. Most of the design parameters in geotechnical LRFD now uses the reliability-based design method.

In this paper, the resistance factors are calibrated and the target reliability index is determined by the first order reliability method (FORM), which was first suggested by Hasofer & Lind (1974). The procedures for calibrating the target reliability index using the FORM is reported in NCHRP Report 507 (Paikowsky et al. 2004).

The component reliability analyses are performed first for the various failure modes which can be occurred in the harbor structures on deep mixed foundations. Limit state functions are defined based on the possible failure modes, i.e. the external failure mode of sliding, failure and bearing capacity of the whole structures, and the internal failure mode of compressive and shear strength of the of DMM foundations (Figure 6).

In the limit state functions, some random variables are used in common to represent the various failure modes. In order to consider the effects of the correlations among the failure modes which comes from using the common random variables, system reliability analysis is also performed. In the case of the foundations in port and harbor structures, the occurrence of one mode of failure could mean the failure of the whole system. Hence, the series system reliability analysis is used.

Using the results of the component reliability analysis by FORM, system probability of failure and the corresponding reliability indices are obtained using Ditlevsen's approach (1979). The equations for bimodal systems used in this study are in Equation 10 and 11.

$$P_f = P\left[(g_i < 0) \cup (g_j < 0)\right] \quad (10)$$

$$P_1 + \sum_{i=2}^k \max\left\{P_i - \sum_{j=1}^{i-1} P_{ij}, 0\right\} \leq P_{system} \leq P_1 + \sum_{i=2}^k \left\{P_i - \max_{j<i} P_{ij}\right\} \quad (11)$$

The correlations among the failure modes are obtained from the unit normal vectors to the zones of failure ( $\alpha_i, \alpha_j$ ) and the intersection angle ( $\theta$ ) at the design points of each failure modes and represented as Equation 12 (Phoon 2008).

$$\rho_{ij} = \alpha_i \cdot \alpha_j = \cos \theta \quad (12)$$

### 5.1 FAILURE MODES AND LIMIT STATE FUNCTIONS in DMM

The failure modes in the improved ground can be divided into the three types: 1) external stability, 2) internal stability and 3) overall stability (Figure 6). The failure modes of the external stability in the wall type DMM are sliding, overturning and bearing capacity failure of the improved ground. The failure modes of internal stability are compressive failure of the improved ground, shear failure of the long and the short walls, and extruding failure of the untreated soils between the walls.

Overall stability check of the whole structure, in which the slip circle failure lines go through the improved grounds, is omitted since the strength of the improved ground is sufficiently high for the circular failure (Kitazume & Nagao 2007). The extruding failure of the untreated soil is also omitted since the safety factors obtained from ASD analysis were much higher than those of the internal stability failure.

In this study, the external failure modes of sliding, failure and bearing capacity of the whole structures, and internal failure mode of compressive and shear strength of the improved ground are selected (Figure 6). Limit state functions for each failure modes are defined in Equation 13-18 using the design external forces of the improved ground shown in Figure 7.

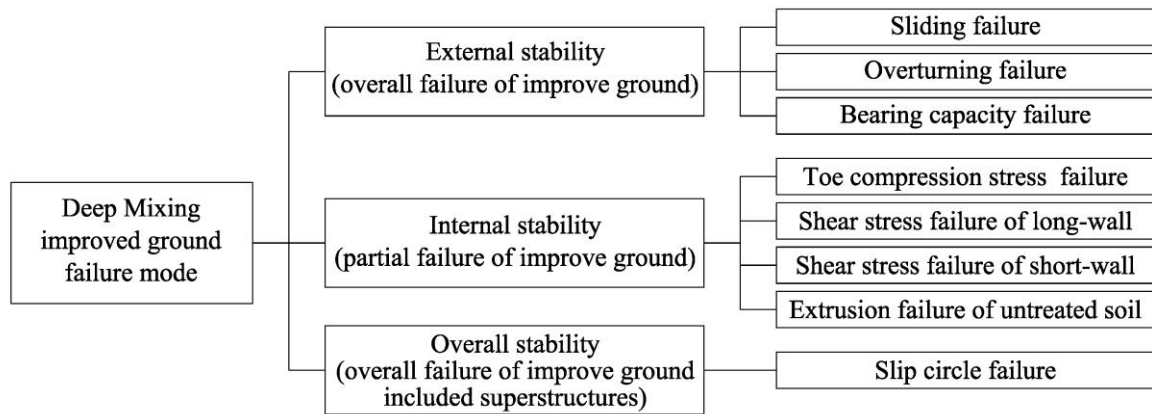


Figure 6. Failure mode for DMM-improved ground.

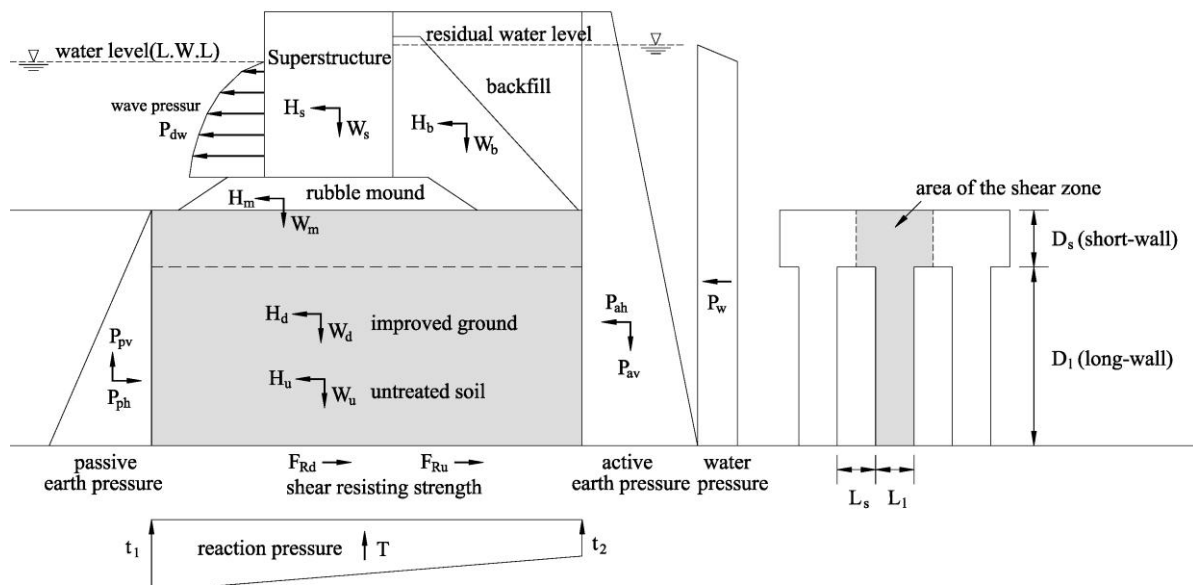


Figure 7. Design loads acting on the improved ground.

### (1) Sliding failure mode

Sliding failure in the improved ground occurs when the horizontal forces acting to the improved ground exceeds the frictional resistances of the underlying soil (Figure 8a). It is defined as the Equation 13.

$$g_1(X) = R - S \quad (13a)$$

$$R = P_{ph} + F_{Rd} + F_{Ru} \quad (13b)$$

$$S = P_{ah} + P_w + P_{dw} \quad (13c)$$

where,  $P_{ah}$  and  $P_{ph}$  are the horizontal active and passive earth pressure,  $F_{Rd}$ ,  $F_{Ru}$  are the shear strength acting on the bottom of the improved ground and untreated soil,  $P_w$  is the residual water pressure,  $P_{dw}$  is the horizontal wave pressure(Figure 8a).

### (2) Overturning failure mode

The overturning failure in improved ground occurs when the driving moment by the forces of active soil pressure, water and wave pressure, etc. exceeds the resistant moment by the self weight of the structure and passive pressure of backfills (Figure 8b). It is defined as Equation 14.

$$g_2(X) = R - S \quad (14a)$$

$$R = W_s x_s + W_m x_m + W_b x_b + W_d x_d + W_u x_u + P_{av} x_{av} \quad (14b)$$

$$S = P_w y_w + P_{dw} y_{dw} + P_{ah} y_{ah} \quad (14c)$$

where  $W_s, W_m, W_b, W_d, W_u$  are the masses of the superstructures, the rubble mound, the backfill material, the treated soil walls, the untreated soil, respectively.  $P_{av}, P_{pv}$  are the vertical cohesive forces of the untreated soil acting on the active and passive side surface.  $x_i$  is the horizontal distance from the vertical force to the front edge of the improved ground,  $y_i$  is the vertical distance from the horizontal force to the bottom of the improved ground.

### (3) Bearing capacity failure mode

The bearing capacity failure occurs when the maximum reaction force ( $t_1$ ) acting on the improved ground exceeds the bearing capacity of the underlying soil (Figure 8c). Since the vertical loads are supported by the long walls, the calculated reaction force is increased by the ratio of the width of long wall. The limit state function is defined as in Equation 15.

$$g_3(X) = R - S \quad (15a)$$

$$R = P_0(1 + N_q) + \frac{1}{2} \gamma_2 L_1 N_r \quad (15b)$$

$$\text{if } e \geq B/6, \quad S = t_1 = \frac{\sum W_i + P_{av}}{B \cdot R_f} \left(1 - \frac{6e}{B}\right) \quad (15c)$$

$$\text{if } e \leq B/6, \quad S = t_1 = \frac{2(\sum W_i + P_{av})}{3X \cdot R_l} \quad (15d)$$

where  $P_0, \gamma'_2$  are the effective stress and the unit weight of the soil under the improved ground.  $L_l$  is the long-wall width (Figure 6),  $B$  is the improved ground width,  $e$  is the eccentric distance,  $W_i$  is the total of the vertical forces,  $X$  is the position of force intensity.  $t_1$  is the reaction pressure at the edge of improved ground.

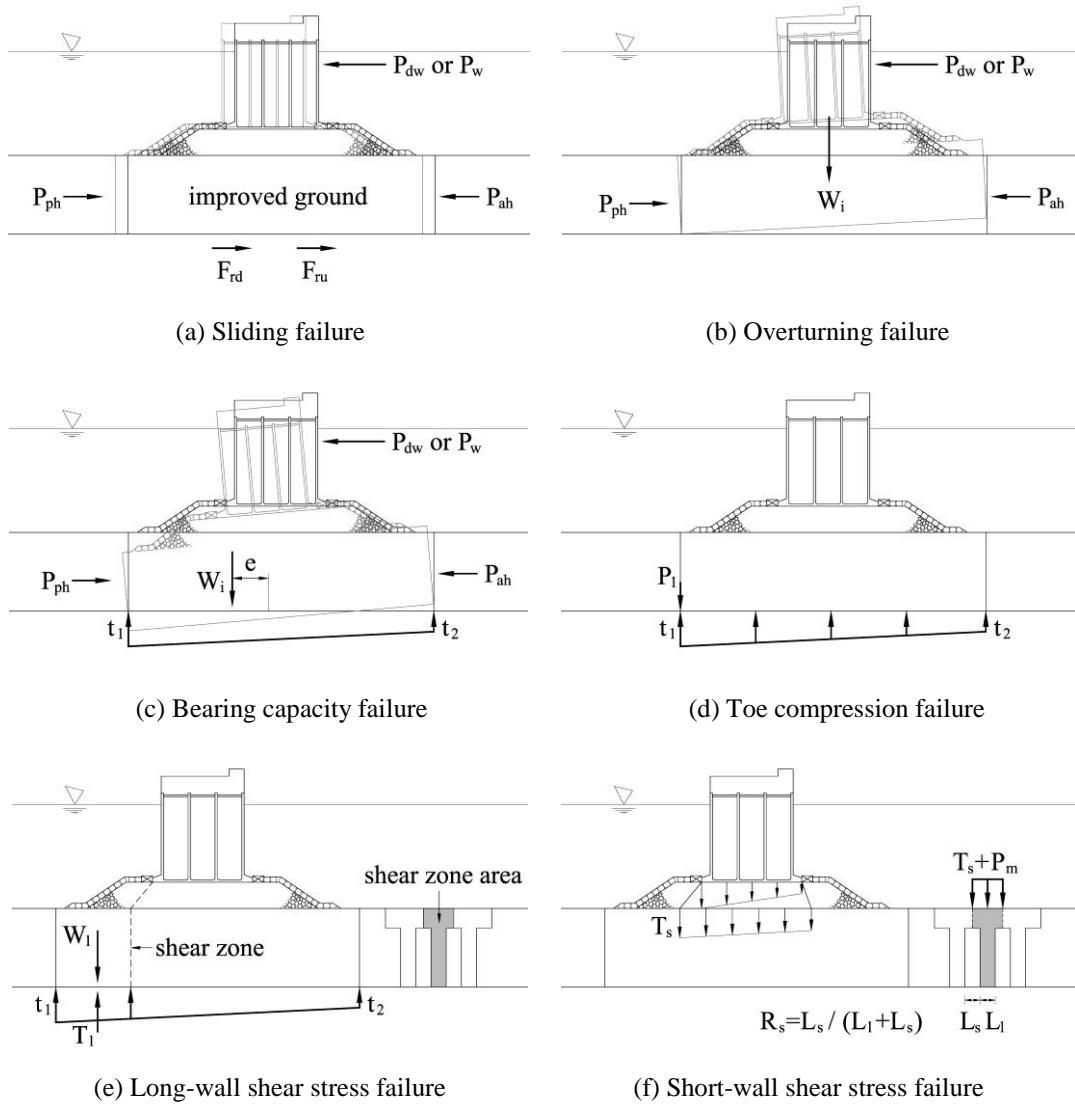


Figure 8. Failure mode for DMM.

#### (4) Toe compression stress failure

The compression failure in the long-wall at the toe occurs when the compression pressure of improved ground,  $T_1$ , exceeds the design standard strength,  $f_c$ .  $T_1$  is the net reaction pressure at the edge of improved ground, which is calculated by subtracting the side skin friction  $P_1$  from  $t_1$  at the toe. The limit state function is defined in Equation 16.

$$g_4(X) = R - S \quad (16a)$$

$$R = f_c = \alpha \cdot \beta \cdot \lambda \cdot q_{ul} \quad (16b)$$

$$S = T_1 = t_1 - P_1 = K_0 \cdot \gamma \cdot h \quad (16c)$$

where  $f_c$  is the design standard strength,  $q_{ul}$  is the unconfined compressive strength of the mixed soil in the laboratory,  $\alpha$ ,  $\beta$ ,  $\lambda$  are the coefficient of effective width of the stabilized column in the field, the reliability coefficient of overlapping, and the ratio of unconfined compressive strength of in-situ stabilized soil column to the mixed soil in the laboratory, respectively.

#### (5) Shear stress failure modes

The maximum shear stresses in the treated soil are developed in vertical faces located just below the upper structure (Figure 8(e)-(f)). The shear stress failure occurs when the maximum shear stresses of long and short wall, ( $T_l, T_s$ ) exceed the strength of the design standard. They are defined as Equation 17 and 18.

For short-wall

$$g_5(X) = R - S \quad (17a)$$

$$R = 1/2 \alpha \cdot \beta \cdot \lambda \cdot q_{ul} \quad (17b)$$

$$S = (T_l - W_l) / A \quad (17c)$$

where  $T_l, W_l$  are the integration of the reaction pressures and the weights of the DM masses from the front edge to the shear zone of the improved ground, respectively. A is the area of the shear zone shown in Figure 6.

For long-wall

$$g_6(X) = R - S \quad (18a)$$

$$R = 1/2 \alpha \cdot \beta \cdot \lambda \cdot q_{ul} \quad (18b)$$

$$S = (T_s + P_m + P_d) \cdot R_s \quad (18c)$$

where  $T_s$  is the distributed vertical pressure from the upper structures to the rubble mound,  $P_m, P_d$  are the weights of the rubble mound and short-wall, respectively.

## 5.2 DETERMINATION OF TARGET RELIABILITY INDEX

Paikowsky et al.(2004) and Kitazume & Nagao(2007) recommended the reliability index obtained from the reliability analysis for the case studies of pre-existing structures of interest as the target reliability index for geotechnical LRFD. In this study, the reliability analyses of the pre-existing structures are performed for the failure modes considered in section 5.1. The reliability levels of the structures in the case studies are estimated and the target reliability index is determined.

Both the component and system reliability analyses are performed using the case studies of domestic harbor structures in recent 5 years, where the DMM is applied for soil improvement under

the foundation. The cases collected are the ones which are the representative structure types in Korea (Table 5). Design data of the cases, i.e. water depth, the width and the depth of the improved walls are also shown in Table 5.

Table 5. Design data used for reliability analysis

| Site           | Design data    |                    |                   |                   |
|----------------|----------------|--------------------|-------------------|-------------------|
|                | Structure Type | Water depth D.L(m) | Improved depth(m) | Improved width(m) |
| A Yeosu(2007)  | Waterbreak     | -14.2              | 24.7              | 66.7              |
| B Namhae(2007) | Quay wall      | -11.7              | 5.6               | 32.3              |
| C Gunsan(2008) | Quay wall      | - 5.3              | 10.0              | 18.1              |
| D Ulsan(2009)  | Waterbreak     | -20.7              | 12.5              | 64.8              |
| E Busan(2010)  | Waterbreak     | -11.2              | 28.4              | 32.5              |

The statistical characteristics of random variables in the limit state functions of the failure modes in the reliability analysis are obtained from the various laboratory and field tests and the literature studies (Table 6).

From the component reliability analyses, the reliability indices for the external and internal failure modes are in the range of  $\beta_c = 5.376\sim 20.251$ , and  $\beta_c = 2.122\sim 7.515$ , respectively. They showed a large difference according to the failure modes. The major failure modes which dominate the stability of the DMM treated soils were the compressive and shear stress failure modes (Table 6). The range of the reliability indices obtained from the system reliability analyses are  $\beta_s = 2.122\sim 3.830$  and are very close to the values of the minimum reliability indices of component analyses in the individual cases. This is because the probabilities of failure for compressive and shear failure modes are significantly higher than those of other failure modes in our case studies. They consist almost with the sum of the probability of failure of the individual failure modes (Equation 11).

Table 6. Statistical model and random variable parameters

| Random variable  |   | Coefficient of variance | Distribution | References              |
|------------------|---|-------------------------|--------------|-------------------------|
| $W_s$            | Masses of the superstructures             | 0.04                    | Normal       | JPHA (2007)             |
| $W_m, W_s$       | Masses of the rubble and backfill         | 0.05                    | Normal       |                         |
| $W_d$            | Masses of the improved ground             | 0.03                    | Normal       | Kitazume & Nagao (2007) |
| $W_u$            | Masses of untreated soil                  | 0.03                    | Normal       |                         |
| $P_{ah}, P_{ph}$ | Horizontal earth pressure                 | 0.10                    | Normal       | Phoon et al. (1995)     |
| $P_{av}, P_{pv}$ | Vertical cohesion force of untreated soil | 0.10                    | Normal       | JPHA (2007)             |
| $P_w$            | Residual water pressure                   | 0.20                    | Lognormal    |                         |
| $P_{dw}$         | Horizontal wave pressur                   | 0.19                    | Lognormal    | Takayama & Ikeda (1994) |
| $\mu$            | Coefficient of friction                   | 0.10                    | Normal       | Nagao (2002)            |
| $f_c$            | Design standard strength of the column    | 0.34                    | Lognormal    | Table 2                 |
| $\gamma_1$       | Unit weight of the untreated soil         | 0.03                    | Normal       | JPHA (2007)             |
| $c_u$            | Undrained strength of the untreated soil  | 0.15                    | Normal       | Lacasse & Nadim (1996)  |
| $N_r, N_q$       | Coefficient of the bearing capacities     | 0.10                    | Normal       | Nagao (2002)            |

The target reliability index in this study is decided based on the system reliability indices as  $\beta_T = 3.1$  and the resistance factors of the internal failure modes are decided based on this index.

Table 7. Comparison of reliability index by component reliability and system reliability analyses

| Site | Component reliability analysis( $\beta_c$ ) |          |          |          |          |          | System reliability Analysis( $\beta_s$ ) |
|------|---|----------|----------|----------|----------|----------|--|
|      | $g_1(X)$                                    | $g_2(X)$ | $g_3(X)$ | $g_4(X)$ | $g_5(X)$ | $g_6(X)$ |  |
| A    | 6.702                                       | 9.075    | 12.733   | 4.102    | 2.353    | 7.515    | $2.353 \leq \beta_s \leq 2.353$          |
| B    | 7.919                                       | 20.251   | 10.813   | 4.600    | 2.122    | -        | $2.122 \leq \beta_s \leq 2.122$          |
| C    | 6.023                                       | 11.853   | 12.945   | 3.830    | 5.897    | -        | $3.830 \leq \beta_s \leq 3.830$          |
| D    | 5.986                                       | 7.759    | 11.371   | 3.796    | 4.926    | 6.142    | $3.796 \leq \beta_s \leq 3.796$          |
| E    | 5.376                                       | 6.184    | 11.594   | 3.403    | 6.244    | 5.404    | $3.403 \leq \beta_s \leq 3.403$          |

## 6 LOAD FACTORS AND LOAD RATIO

In the field of the structural engineering, many researchers spent time to predict the reliable loads on the social infra structures for LRFD application. As the result, the load factors and their statistical characteristic values are determined from the cumulated database.

For port and harbor structures, it seems proper to use the environmental load factor, e.g. wave load, as the load factor. In Table 8, the load factors and their statistical values are introduced based on the design standards of port and harbor in Korea (KPHA 2005) and API (1993), in which the environmental load factors are treated in depth. Hence, the live load factors in the basic equation of LRFD i.e. Equation 8, are treated as the environmental load factors in this study, and the resistance factors are decided.

Table 8. Values of load factors and statistical properties assumed for calibration of resistance factor

| Loads     | Load factors       | Statistical value for loads |                         |
|-----------|--------------------|-----------------------------|-------------------------|
|           |                    | Bias factors                | Coefficient of variance |
| Dead load | $\gamma_{QD}=1.10$ | $\lambda_{QD}=1.00$         | $COV_{QD}=0.10$         |
| Live load | $\gamma_{QL}=1.30$ | $\lambda_{QL}=0.91$         | $COV_{QL}=0.19$         |

Load ratio is defined as the ratio of the dead load and live load, i.e.  $Q_D/Q_L$ . It is known that the sensitivity of the reliability index is low to the load ratio. In the bridge structures, the load ratio is usually determined based on the span length of the bridges, and the range of the load ratio is determined in  $Q_D/Q_L = 0.5 \sim 4.0$ . In this study, the load ratios are calculated based on the design loads of 5 case studies referred in Table 5, and listed in Table 9. Although the load ratio is distributed in rather wide ranges, its range is in between 2.9~4.4 except the site B. This result is similar to the case of bridge structures.

Table 9. Loads ratio calculated in this study

| Site                     | A   | B    | C   | D   | E   |
|--------------------------|-----|------|-----|-----|-----|
| Loads ratio( $Q_D/Q_L$ ) | 4.4 | 12.2 | 4.0 | 3.3 | 2.9 |

## 6 CALIBRATION OF RESISTANCE FACTORS

### 6.1 PRELIMINARY CALIBRATION SCHEME USING SAFETY FACTOR

FHWA(2001) suggested the a preliminary calibration scheme in Equation 19 to calculate the resistance factors using the safety factor in ASD. To compare the calibration scheme using reliability based design, a preliminary calibration scheme using safety factors is performed in this section.

$$\phi = \frac{\gamma_{QD}Q_D + \gamma_{QL}Q_L}{F_s(Q_D + Q_L)} = \frac{\gamma_{QD}(Q_D/Q_L) + \gamma_{QL}}{F_s(Q_D/Q_L + 1)} \quad (19)$$

The load ratio and the load factors in this analysis are as adopted from Table 8-9. The safety factors in the application of DMM to port and harbor structures according to the ASD are  $F_s = 1.2$  for sliding and overturning failure modes and  $F_s=3.0$  for bearing capacity, Toe compression stress and shear stress failure modes.

The calculated resistance factors are listed by varying the load factors in Table 10. It can be recognized that the resistance factors are slightly decreased when the  $Q_D/Q_L$  is less than 2.0 and converged to constant values thereafter (Figure 9). In the range of  $Q_D/Q_L = 2.9\sim 4.4$  for DMM treated grounds, the results turns out that the resistance factor,  $\phi$ , is 0.95 for  $F_s = 1.2$  and  $\phi = 0.38$  for  $F_s = 3.0$ .

Table 10. Resistance factors based on the factors of safety

| Failure mode   | Factors of safety | Resistance factors |               |               |                |
|--|-------------------|--------------------|---------------|---------------|----------------|
|  |                   | $Q_D/Q_L=1.0$      | $Q_D/Q_L=2.0$ | $Q_D/Q_L=4.0$ | $Q_D/Q_L=10.0$ |
| Sliding<br>Overturning                                     | $F_s=1.2$         | 1.00               | 0.97          | 0.95          | 0.93           |
| Bearing capacity<br>Toe compression stress<br>Shear stress | $F_s=3.0$         | 0.40               | 0.39          | 0.38          | 0.37           |

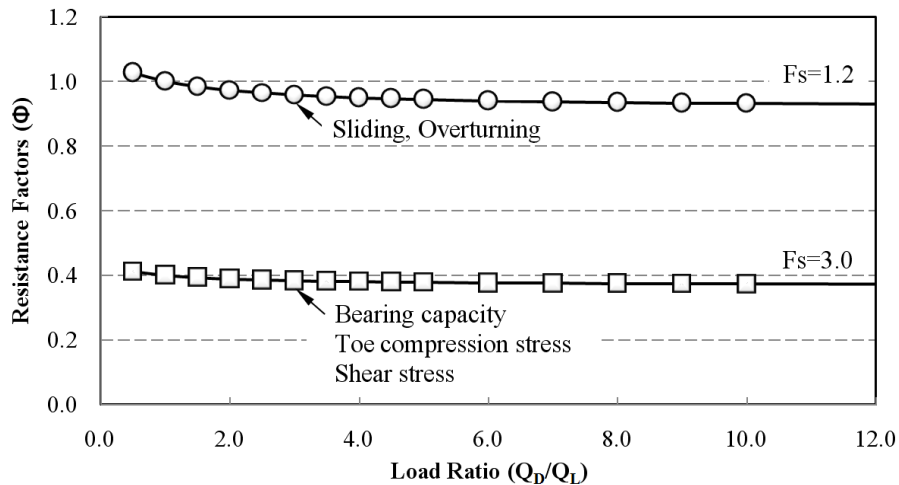


Figure 9. Resistance factors as function of load ratio and safety factors.

## 6.2 CALIBRATION BASED ON TARGET RELIABILITY INDEX

The resistance factors are calculated according to the reliability based LRFD calibration scheme. The results of the analysis of the compressive strength data for DMM treated construction sites and the target reliability indices from the reliability analyses of the existing harbor structures founded on the DMM treated soils, in this study, are used. The statistical values for the loads and resistances obtained from the calibration process are summarized in Table 11.

The calculated results of the resistance factors with respect to the load ratio and the target reliability indices are shown in Figure 10 and Table 12. The resistance factors are decreased as the load ratios are increased. As the target reliability indices are increased, the spread of the resistance factors are slightly decreased relating to the load ratios. Within the load ratio of  $Q_D/Q_L=2.9\sim 4.4$ , the resistance factors are almost the same and have 2% difference between max. and min. values.

Within the ranges of the reliability index of the existing sites,  $\beta_s=2.12\sim 3.83$ , and the ranges of the load ratio,  $Q_D/Q_L=2.9\sim 4.4$ , the resistance factors are calculated as  $\phi=0.33\sim 0.66$ . In the case of the target reliability index  $\beta_T=3.1$ , the resistance factor is calculated as  $\phi=0.44\sim 0.45$ .

Table 11. Statistical value for reliability-based on calibration of resistance factors for internal stability of DMM

| Load               |                     |                 | Resistance       |              | Target Reliability index                     |
|--------------------|---------------------|-----------------|------------------|--------------|--|
| Load factors       | Bias factors        | COV             | Bias factor      | COV          |  |
| $\gamma_{QD}=1.10$ | $\lambda_{QD}=1.00$ | $COV_{QD}=0.10$ | $\lambda_R=1.36$ | $COV_R=0.35$ | $\beta_T=3.1$<br>( $\beta_s=2.12\sim 3.83$ ) |
| $\gamma_{QL}=1.30$ | $\lambda_{QL}=0.91$ | $COV_{QL}=0.19$ |                  |              |  |

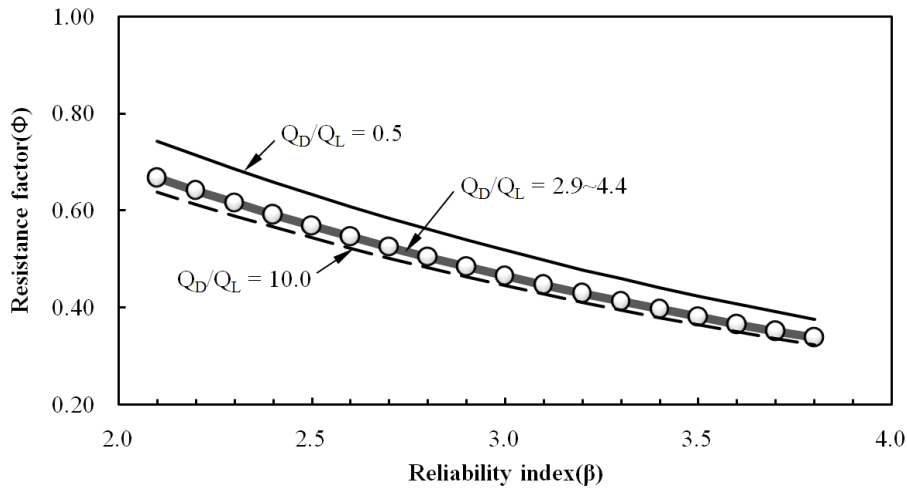


Figure 10. Resistance factors for reliability index.

Table 12. Result of calibration of resistance factors for internal stability of DMM

| Reliability index | Resistance factors |               |               |                |
|-------------------|--------------------|---------------|---------------|----------------|
|                   | $Q_D/Q_L=0.5$      | $Q_D/Q_L=2.9$ | $Q_D/Q_L=4.4$ | $Q_D/Q_L=10.0$ |
| $\beta = 2.12$    | 0.74               | 0.66          | 0.65          | 0.63           |
| $\beta = 2.33$    | 0.68               | 0.61          | 0.60          | 0.58           |
| $\beta = 2.50$    | 0.63               | 0.57          | 0.56          | 0.54           |
| $\beta = 3.00$    | 0.52               | 0.46          | 0.46          | 0.44           |
| $\beta_T = 3.10$  | 0.50               | 0.45          | 0.44          | 0.43           |
| $\beta = 3.50$    | 0.42               | 0.38          | 0.37          | 0.36           |
| $\beta = 3.83$    | 0.37               | 0.33          | 0.33          | 0.32           |

## 7 CONCLUSIONS

In this study, the uncertainties of the load and resistances on the improved grounds by DMM are analyzed statistically. Target reliability indices are determined based on both component and system reliability analyses. The calibrations of the resistance factors for the internal stability failure modes of the DMM improved harbour structures are performed. The results obtained are the following:

- (1) The compressive strength of the domestic DMM improved grounds ( $q_{uf}$ ) is about 85% of the compressive strength of the laboratory manufactured DMM samples ( $q_{ul}$ ), i.e.  $q_{uf} / q_{ul} = 0.85$ . The Coefficient of variance (COV) of  $q_{uf}$  was obtained as 0.34.
- (2) The bias factor of resistance of DMM improved ground is defined as the ratio of  $q_{uf}$  versus the strength of the design standards ( $q_{uck}$ ). The bias factor and the COV of the resistance are calculated as  $\lambda_R = 1.36$  and  $COV_R = 0.35$ .
- (3) The results of goodness-of-fit test for the bias data of the resistance show that both the normal and lognormal distributions are satisfied the criteria. It seems that the lognormal distribution is more proper to the analysis of this study.
- (4) The reliability indices from the component reliability analysis for DMM treated soils are located in the range of  $\beta_e = 2.12 \sim 20.25$ . They have large discrepancies depending on the failure modes. The dominant failure modes in the DMM treated soils are turned out to be compressive strength at the toe of the improved ground and the shear strength of the improved ground.
- (5) The range of the reliability indices obtained from the system reliability analyses is  $\beta_s = 2.12 \sim 3.83$  and is dominated by the dominant failure modes. The target reliability index is suggested as  $\beta_T = 3.1$  by averaging the reliability indices from the reliability analyses of the existing five field studies.
- (6) The resistance factors of the port and harbor structures improved by DMM were calculated from the load factors and the related statistical analysis. Within the calculated reliability range of the existing structures, i.e.  $\beta_s = 2.122 \sim 3.830$  and the range of the load ratio ( $Q_D / Q_L$ ) 2.9~4.4, the resistance factors are obtained as  $\phi = 0.33 \sim 0.67$ . In the case of the target reliability index  $\beta_T = 3.1$ , the resistance index is calculated as  $\phi = 0.43 \sim 0.44$ .
- (7) It is expected that the suggested resistance factors would be useful for the geotechnical engineers to design the port and harbor structures on the DMM improved grounds which have large uncertainties of the random variables in load and resistance.

## ACKNOWLEDGEMENTS

This research was supported by the Basic Science Research Program through the National Research Foundation of Korea (NRF), funded by the Ministry of Education, Science and Technology (No.2012-0002408).

This paper is also a part of the result from the "Maintenance of Foundation Design Criteria under the Construction Facilities for Standardization", the "Construction & Transportation R&D Policy and Infrastructure Project".

## REFERENCES

- AASHTO (2010). AASHTO LRFD Bridge Design Specifications. Fifth Edition, American Association of State Highway and Transportation Officials, Washington, D.C.
- Allen, T. M., Christopher, B. R., Elias, V. & DiMaggio, J. (2001). Development of the Simplified Method for Internal Stability of Mechanically Stabilized Earth(MSE) Walls. Washington State Department of Transportation, Report WA-RD 513, pp. 108.
- Allen, T. M., Nowak, A. S. & Bathurst, R. J. (2005). Calibration to Determine Load and Resistance Factors for Geotechnical and Structural Design. Transportation Research Board, Circular Number E-C079, Washington, D.C.
- API (1993). Draft Recommended Practice for Planning, Designing and Constructing Fixed Offshore Platforms—Load and Resistance Factor Design. API RP2A-LRFD, American Petroleum Institute, Dallas, TX.
- Barker, R. M., Duncan, J. M., Rojiani, K. B., Ooi, P. S. K., Tan, C. K. & Kim, S. G. (1991). NCHRP Report 343: Manuals for the Design of Bridge Foundations. Transportation Research Board, National Research Council, Washington, DC.
- CDIT (2002). The Deep Mixing Method-Principle. Design and Construction, Coastal Development Institute of Technology (CDIT), Japan, Balkema, pp. 76-77.
- CEN (2004). Eurocode7-Geotechnical Design. European Committee for Standardization, TC250.
- Chen, Y. (2000a). Practical Analysis and Design Methods of Mechanically Stabilized Earth Walls I: Design Philosophies and Procedures. *Engineering Structures*, 22(7), pp. 793–808.
- Chen, Y. (2000b). Practical Analysis and Design Methods of Mechanically Stabilized Earth Walls II: Design Comparisons and Impact of LRFD Method. *Engineering Structures*, 22(7), pp. 809–830.
- CSA (2006). Canadian Highway Bridge Design Code. CAN/CSA Standard S6-06, CSA International, Rexdale, Ontario.
- D'Appolonia (1999). Developing New AASHTO LRFD Specification for Retaining Walls. Final Report, NCHRP Project 20-7, Task 88, Ground Technology, Inc., Monroeville, PA, pp. 50.
- DGI (1985). Code of Practice for Foundation Engineering. Danish Geotechnical Institute, Copenhagen, Denmark.
- Ditlevsen, O. (1979). Narrow Reliability Bounds for Structural Systems. *Journal of Structural Mechanics*, 7(4), pp. 453-472.
- DIN EN (2009). 1997-1 Eurocode 7: Geotechnical Design - Part 1: General Rules. German Institute for Standardization.
- DS/EN (2007). 1997-1 Eurocode 7: Geotechnical Design - Part 1: General Rules. Danish Standards.
- Fellenius, B.(1994). Limit States Design for Deep Foundations. Proceedings U.S. DOT International Conference on Deep Foundations, Orlando, Federal Highway Commission.
- FHWA (2001). Load and Resistance Factor Design(LRFD) for Highway Bridge Structures. FHWA HI-98-032, Federal Highway Administration, U.S. Department of Transportation, pp. 3-7.
- Hasofer, A. M. & Lind, L. C. (1974). Exact and Invariant Second Moment Code Format. *Journal of the Engineering Mechanics Division*, ASCE, 100(1), pp. 111-121.
- Hamilton, J. & Murff, J. (1992). Selection of LRFD Resistance Factors for Pile Foundation Design. Proceedings Structures Congress '92, American Society of Civil Engineers Structures Congress, April 13–15, San Antonio, Texas.
- Huang, B. Q. (2010). Numerical Study and Load Resistance Factor Design(LRFD) Calibration for Reinforced Soil Retaining Walls. Ph. D. Thesis, Queen's University, Canada.
- JPHA (2007). Technical Standards and Commentaries of Port and Harbor Facilities in Japan. Japan Port and Harbor Association(in Japanese).
- Kawasaki, T., Saitoh, S., Suzuki, Y. & Babasaki, T. (1984). Deep Mixing Method using Cement Slurry as Hardening Agent. Seminar on Soil Improvement and Construction Techniques in Soft Ground, Singapore, pp. 17-38.
- Kwak, K. S., Kim, K. J., Huh, J., Lee, J. H. & Park, J. H. (2010). Reliability based calibration of resistance factor for static bearing capacity of driven piles. *Canadian Geotechnical Journal*, 47(5), pp. 528-538.
- KGS (2009). Design Standard for Structural Foundation and Commentaries, Korea Geotechnical Society, certified Ministry of Land, Transport and Maritime Affairs in Korea(in Korean).
- KICT (2008). Determination of Resistance Factors for Foundation Structure Design by LRFD. Korea Institute of Construction Technology(in Korean).
- Kim, D. W. & Lee, J. W. (2012). Resistance Factor Contour Plot Analyses of Load and Resistance Factor Design of Axially-loaded Driven Piles in Clays. *Computers and Geotechnics*, 44, pp. 9-19.
- Kitazume, M. & Nagao, T. (2007). Studies of Reliability based Design on Deep Mixing Improved Ground. Report of Port and Airport Research Institute, 46(1), pp. 3-44.
- KPHA (2005). Design Standard for Port and Harbor. Korea Port and Harbor Association, certified Ministry of Land, Transport and Maritime Affairs in Korea(in Korean).
- Kulhawy, F. H. & Phoon, K. K. (2002). Observations on Geotechnical Reliability-Based Design Development in North America. Foundation Design Code and Soil Investigation in View of International Harmonization and Performance Based Design, Proceedings of the IWS Kamakura 2002 Conference, Japan, pp. 31-48.
- Lacasse, S. & Nadim, F. (1996). Uncertainties in Characterizing Soil Properties. Proceedings of Uncertainty in the Geologic Environment: From Theory to Practice, 1, ASCE, pp. 49-75.
- Lazarte, C. A. (2011). NCHRP Report 701: Proposed Specifications for LRFD Soil-Nailing Design and Construction. Transportation Research Board, Washington, D.C.

- Meyerhof, G. (1994). Evolution of Safety Factors and Geotechnical Limit State Design. Second Spencer J. Buchanan Lecture, Texas A&M University, 4, pp. 32.
- Nagao (2002). Reliability Based Design Method for Checking the External Safety of Caisson Type Breakwaters, Research Report of NILIM, No. 4(in Japanese).
- NBN EN (2005). 1997-1: Eurocode 7: Geotechnical Design - Part 1: General Rules . Belgian Standards.
- NF EN (2005). 1997-1, Eurocode 7: Geotechnical Design – Part 1: General Rules. Association Francaise de Normalisation.
- Nowak, A. S. (1999). NCHRP Report 368: Calibration of LRFD Bridge Design Code. Transportation Research Board, National Research Council, Washington, D.C.
- Okahara, M., Fukui, J., Shirato, M., Matsui, K., & Honjo, Y. (2003). National Report on Geotechnical Codes in Japan. Proc. 12th Asian Regional Conference on Soil Mechanics and Geotechnical Engineering
- O'Neill, M. (1995). LRFD Factors for Deep Foundations through Direct Experimentation. Proceedings of US/Taiwan Geotechnical Engineering Collaboration Workshop, Sponsored by the National Science Foundation(USA) and the National Science Council(Taiwan, ROC), Taipei, January 9–11, pp. 100–114.
- Paikowsky, S., Birgisson, G., McVay, M., Nguyen, T., Kuo, C., Baecher, G., Ayyub, B., Stenerson, K., O'Mally, K., Chernauskas, L. & O'Neill, M. (2004). NCHRP Report 507: Load and Resistance Factor Design(LRFD) for Deep Foundations. Transportation Research Board of the National Academies, Washington, DC.
- Paikowsky, S. G., Canniff, M. C., Lesny, K., Kisse, A., Amatya, S. & Muganga, R. (2010). NCHRP Report 651: LRFD Design and Construction of Shallow Foundations for Highway Bridge Structures. Transportation Research Board of the National Academies, Washington, DC.
- Phoon, K. K., Kulhawy, F. H. & Grigoriu, M. D. (1995). Reliability-Based Design of Foundations for Transmission Line Structures. Electric Power Research Institute, Palo Alto, Report TR-105000.
- Phoon, K. K. (2008). Reliability-Based Design in Geotechnical Engineering: Computations and Applications. Numerical Recipes for Reliability Analysis – a Primer., eds. by Phoon, K. K., Taylor & Francis, pp. 1-76.
- Suzuki, Y. (1982). Deep Chemical Mixing Method using Cement as Hardening Agent. Symposium on Soil and Rock Improvement, Bangkok, pp. 1.1-1.24.
- Takayama, T. & Ikeda, T. (1994). Estimation of Encounter Probability of Sliding for Probabilistic Design of Breakwater. Proceedings of the Wave Barriers in Deepwaters, Port and Harbour Research Institute, Yokosuka, pp. 438-457.
- Taki, O. (2003). Strength Properties of Soil Cement Produced by Deep Mixing. ASCE, Geotechnical Special Publication, No. 120, PP. 646-657.
- Tang, W. (1993). Recent Developments in Geotechnical Reliability. Proceedings of the Conference on Probabilistic Methods in Geotechnical Engineering, Canberra, Australia, Balkema, Rotterdam, Netherlands, pp. 3–28.
- Withiam, J. L., Voytko, E. P. & Kelly, B. C. (1995). Section 10, Foundations; Section 11, Abutments, Piers and Walls; Section 12, Buried Structures of Design Manual 4. Exception Specifications AASHTO LRFD Specification for the Pennsylvania Department of Transportation.
- Withiam, J., Voytko, E., Barker, R., Duncan, M., Kelly, B., Musser, S., & Elias, V. (1998). Load and Resistance Factor Design(LRFD) of Highway Bridge Substructures. FHWA HI-98-032, FHWA.
- Yoon, H. J., Jung, S. J. & Kim, M. M. (2007). Resistance factors for drilled shafts embedded in weathered rock. Korean Geotechnical Society, Journal of Geotechnical Engineering, 23(8), pp. 107-116(in Korean).
- Zhang, L. M., Liu, J. L. & Zhang, Z. M. (2003). The Chinese Limit State Design Code for Building Pile Foundations JGJ 94-94: A Comparative Study. Proceeding of the International Workshop on Limit State Design in Geotechnical Engineering Practice, Massachusetts Institute of Technology, U.S.A.